Soil Dynamics and Earthquake Engineering 190 (2025) 109162

Contents lists available at ScienceDirect

Soil Dynamics and Earthquake Engineering

journal homepage: www.elsevier.com/locate/soildyn

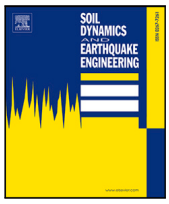

Technical note

Response of an elastic half-plane with an embedded circular cavity subject to a harmonic anti-plane shear wave: A comparison of methods

Mingjuan Zhao *, João Manuel de Oliveira Barbosa, Andrei V. Metrikine, Karel N. van Dalen

Faculty of Civil Engineering and Geosciences, Delft University of Technology, Stevinweg 1, 2628 CN, Delft, The Netherlands

ARTICLE INFO

Keywords:
Cavity in half-plane
SH wave
Comparison study
Method of images
Method of conformal mapping
Indirect BEM

ABSTRACT

In this paper, we investigate the response of a cavity embedded in an elastic half-plane (2D) subjected to a harmonic SH wave. In previous work, the method of conformal mapping and the indirect boundary element method (indirect BEM) were employed to solve the 3D wave scattering from a cylindrical tunnel embedded in a half-space. Inaccurate results were obtained particularly at high frequencies (method of conformal mapping). Therefore, in this study we focus on a comparison of the two methods with the method of images, which serves as a benchmark solution. Through a systematic evaluation, we confirm that the two methods accurately work within the complete considered ranges of the dimensionless frequency and the embedded cavity depth. This suggests that representing the waves scattered from the free surface by cylindrical waves in the method of conformal mapping is the cause of the inaccuracies at high frequency in the 3D problem; the cylindrical waves are probably not able to fully capture all wave conversions taking place at the free surface. The presented results reveal significant effects of the system parameters on the responses. The system's response curves display nearly equally spaced resonances, which is in line with those of the 1D shear layer subject to bedrock motion, while similar response curves for the 3D case do not have this feature.

1. Introduction

The dynamics of underground structures, including cavities and tunnels, has been a crucial research topic in civil engineering and earthquake engineering [1]. In our previous work, we utilised the method of conformal mapping to address the 3D wave scattering problem from a cylindrical tunnel embedded in a half-space, as well as the indirect BEM [2]. However, it was observed that inaccurate results may arise using the former method, particularly for high-frequency loadings. As pointed out in [2], the reason for the inaccuracy probably lies in the fact that the secondary scattered waves in the soil (i.e., waves first scattered from the tunnel and then reflected from the free surface of the half-space) are represented by cylindrical waves and not by plane waves, while the latter are most likely more suitable to represent the responses at the flat ground surface at high frequencies. This observation motivates the current study, where we aim to verify the accuracy of the method of conformal mapping and of the indirect BEM. To achieve this, we conduct a comparative analysis involving three methods: the method of images, the method of conformal mapping and the indirect BEM. We focus on the simple 2D problem of a circular cavity embedded in an elastic half-plane subject to harmonic plane SH waves. As the considered model is two dimensional, the geometry is regular, and the excitation is an anti-plane shear wave, closed-form solutions can be obtained using the method of images. These serve as benchmark results for evaluating the outcomes obtained by the other two methods. Our study aims to validate the accuracy of the method of conformal mapping and the indirect BEM, through a systematic evaluation encompassing a large range of system parameters. Such a comprehensive evaluation of the method of conformal mapping and the indirect BEM for the 2D anti-plane shear wave case has not been undertaken previously.

This paper is organised as follows. Sections 2 and 3 provide a statement of the problem under consideration and specify the methods, respectively. Section 4 presents convergence tests of the three methods and a comprehensive evaluation of their accuracy. Specifically, we analyse the accuracy with respect to varying dimensionless frequency and the embedded depth of the cavity. Additionally, we briefly interpret the obtained system responses. Finally, Section 5 summarises the conclusions of this study.

2. Problem statement

2.1. Model description

In this paper, we consider the 2D problem of a cylindrical cavity embedded in an elastic half-plane subject to a harmonic SH wave; see

* Corresponding author.
E-mail address: mingjuanzhao87@gmail.com (M. Zhao).

https://doi.org/10.1016/j.soildyn.2024.109162
Received 29 May 2024; Received in revised form 30 October 2024; Accepted 2 December 2024
Available online 20 December 2024

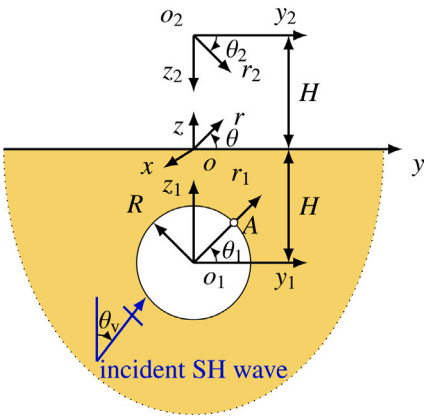

Fig. 1. Model of a circular cavity embedded in an elastic half-plane subjected to a harmonic anti-plane shear wave.

Fig. 1. The half-plane is modelled by an elastic continuum, which is assumed to be linear, elastic, homogeneous and isotropic. To facilitate the analysis, we employ three coordinate systems (like in [2]). The image of the cavity is symmetrically positioned with respect to the free surface. The centre of the cavity, denoted as o_1, is located beneath the free surface at a depth of H, and its radius is represented by R. We define the vertical incident angle, θ_v, as the angle between the wave propagation direction and the positive vertical z axis.

2.2. Governing equation and boundary conditions

Considering our focus on the steady-state solution to the 2D anti-plane problem, we assume that both the excitations and responses of the system are harmonic and proportional to $e^{+i\omega t}$; i denotes the imaginary unit, t represents time, $\omega = 2\pi f$ is the angular frequency, and f is the frequency in Hz. For brevity, we omit the factor $e^{+i\omega t}$ in all subsequent expressions. The governing equation of motion of the soil medium in the frequency domain, in the absence of external forces, reads [3,4] $\mu\nabla^2 u = -\omega^2\rho u$, where the symbols μ and ρ signify the shear modulus and density of the soil, respectively; the operator ∇^2 denotes the 2D Laplace operator. The variable u denotes the anti-plane displacement in the x direction.

The system is excited by seismic wave originating from beneath the cavity. Consequently, a stress-free boundary condition is imposed at both the free surface of the half-plane and the cavity surface: $\sigma_{zx} = 0$ and $\sigma_{r_1 x_1} = 0$, respectively.

3. Methods

Details related to the method of conformal mapping and the indirect BEM can be found in [2,5], respectively. As explained in [2], the presence of the cavity induces the scattering, resulting in the generation of directly scattered cylindrical waves denoted as $u_{s,1}$. The secondary scattered waves, $u_{s,2}$, arise when the directly scattered waves encounter the free surface of the half-space.

For the method of conformal mapping, the scattered wave fields are given as follows [2]:

$$u_{s,1} = \sum_{n=-\infty}^{\infty} a_n H_n^{(2)}\left(k_S r_1\right)\exp\left(\mathrm{i}\, n\theta_1\right), \tag{1}$$

$$u_{s,2} = \sum_{n=-\infty}^{\infty} b_n H_n^{(2)}\left(k_S r_2\right)\exp\left(\mathrm{i}\, n\theta_2\right), \tag{2}$$

where $k_S = \omega/c_S$ denotes the wavenumber of the SH wave, and $c_S = \sqrt{\mu/\rho}$ is the velocity of the shear wave. It is important to note that while the method of images can be applied to the 2D anti-plane shear problem under consideration, it is not applicable to more complex problems such as 2D plane-strain and 3D cases. In our previous work, we combined the method of conformal mapping and the spirit of the method of images to address these more complex problems, and choosing the coefficients of the primary and secondary scattered fields differently was a necessity [2,6]. For that reason, a_n and b_n are not chosen the same a priori in the current analysis either. It will enable us to check the accuracy of the conformal mapping method for this simple problem; as stated before (Section 1), for the 3D problem, inaccuracies were observed at high frequencies [2].

In the traditional application of the method of images, b_n is set equal to a_n. Through numerical analysis, it can be verified that b_n is nearly exactly the same as a_n when applying the method of conformal mapping. This proofs the validity and accuracy of the method of conformal mapping as well as its implementation.

For the indirect BEM, we use the 2D Green's functions based on the 2.5D Green's functions of a full-space and a half-space, like in our previous work [5]. The 2D case can be obtained by setting $k_x = 0$ in the relevant expression given in [5]; k_x is the wavenumber in the longitudinal direction.

Table 1
The required number of circumferential modes N or the number of source and receiver points (N_s, N_r) to achieve converged results for different methods and different dimensionless frequencies. Note that method 1, 2 and 3 represents the method of images, the method of conformal mapping and the indirect BEM, respectively.

Methods	$\eta = 0.5$	$\eta = 1.0$	$\eta = 2.0$	$\eta = 3.0$
Method 1	$N = 3$	$N = 6$	$N = 10$	$N = 12$
Method 2	$N = 5$	$N = 6$	$N = 10$	$N = 13$
Method 3	(20, 40)	(40, 80)	(60, 120)	(60, 120)

4. Convergence tests and comprehensive evaluation

In the subsequent presentation of results, the normalised anti-plane displacement and shear stress are used: $U = u/u_0$ and $\Sigma_{\theta_1 x_1} = \sigma_{\theta_1 x_1}/\left(\omega\rho c_S u_0\right)$ (like in [2]), where u_0 is the amplitude of the displacement associated with the incident SH wave.

It can be verified that the results obtained using the three methods align well with the results in the literature [7]. In this paper, the parameters of the soil medium are taken as follows: $E = 3.26 \times 10^7$ Pa and $\rho = 1932$ kg/m^3. The geometry of the cavity is as follows: $R = 5$ m and $H/R = 1.5$. The dimensionless frequency is defined as $\eta = \omega R/\left(\pi c_S\right)$ like in [7].

4.1. Convergence tests

In this section, we present convergence tests of the three methods. The considered parameters are $H/R = 5.0$ and $\theta_v = 0^\circ$. In Table 1, we observe that both the method of images and the method of conformal mapping achieve convergence with a small number of circumferential modes. At dimensionless frequencies of 0.5 and 3.0, the method of conformal mapping requires two and one additional circumferential modes compared to the method of images, respectively. This indicates that the method of images may converge faster. The reason is that the accuracy of the method of images is higher. The computed a_n and b_n turn out to be very close but not exactly the same in the method of conformal mapping, which is a result of small inaccuracies in the corresponding matrix inversion.

Regarding the computational time, the results demonstrate that the method of images exhibits slightly higher efficiency compared to the method of conformal mapping. On the other hand, the indirect BEM needs significantly more computational time, making it the least efficient among the three methods.

4.2. Comprehensive evaluation

As discussed above, all three methods can demonstrate accurate performance for the individual frequencies considered. However, for the 3D problem [2], it has been shown that accurate results cannot be obtained at high frequencies using the method of conformal mapping while the indirect BEM does. In this section, we further investigate the accuracy of the method of conformal mapping and the indirect BEM within specified ranges of the dimensionless frequency and the embedded depth. The solutions obtained by the method of images are taken as the benchmark. The base-case parameters are set as $\eta = 0.5$, $H/R = 5.0$ and $\theta_v = 0^\circ$. In the following analysis, we present the maximum absolute value of U at the ground surface within the range $y/R = [-4, 4]$, as well as the maximum absolute values of $\Sigma_{\theta_1 x_1}$ at the cavity surface.

4.2.1. Dimensionless frequency

The considered dimensionless frequencies are in the range of $\eta = 0.002 - 3.0$, corresponding to $f = 0.16 - 244.85$ Hz, which covers the seismic range as well as higher-frequency loadings. Fig. 2 illustrates that the results obtained by the three methods coincide, indicating accurate performance of the method of conformal mapping and the indirect BEM. In contrast to the 3D case [2], the method of conformal mapping demonstrates accurate behaviour at high frequencies for the 2D SH problem under consideration. The discrepancy can be attributed to the fact that the secondary scattered waves in the soil are represented by cylindrical waves originating from the image source, and not by plane waves, while the latter are most likely more suitable to represent the response (in the 3D case) at the flat ground surface at high frequencies and fully capture all wave conversions taking place; the relatively poor representation leads to a larger condition number of the matrix that needs to be inverted, which yields to inaccurate results. In any case, we can ascertain the accuracy of the method of conformal mapping and the indirect BEM for the current problem, as the obtained the results align with the closed-form solutions.

The frequency-response curves are shown in Fig. 2; we observe many resonances, some of which are a bit more pronounced than others. Fig. 2(a) illustrates that the first two peak values (though not the most pronounced ones) occur at $\eta = 0.09$ and $\eta = 0.27$ for the ground surface displacement U. Fig. 2(b) demonstrates two prominent peaks at the same frequencies for the shear stress $\Sigma_{\theta_1 x_1}$. Furthermore, we observe that the resonances are nearly equally spaced, which is very similar to the result for the well-known one-dimensional (1D) shear layer subject to bedrock motion shown in the book by Kramer [8]. The resonances in the 1D model are predicted by $\cos(k_S L) = 0$, where L is the thickness of the soil layer; this leads to the expression for the resonance frequencies $\omega_n = (\pi/2 + n\pi)c_S/L$, n being a positive integer. Note that for the considered scenario, the thickness of the soil layer above the cavity is $L = H - R = 4R$. The corresponding dimensionless resonance frequencies can be easily derived, and their spacing turns out to be 0.25 ($\Delta\omega = \pi c_S/L$, so that $\Delta\eta = \Delta\omega R/(\pi c_S) = R/L = 1/4$). This is in line with Fig. 2; see for example the distance between the peaks in the range of $(1 - 2)$ in Fig. 2 (b).

4.2.2. Embedded depth of the cavity

We consider the range of embedded depth ratios from 1.5 to 20. Fig. 3 demonstrates that the three methods yield consistent results, indicating that the method of conformal mapping and the indirect BEM work accurately.

Fig. 3 demonstrates that both the responses at the ground surface and at the cavity surface oscillate as the embedded depth increases. Different nearly equally spaced resonances can be observed, like in Fig. 2. The spacing between resonances is approximately equal to 2. To understand the resonances at different frequencies, we examine the responses of the system at frequencies of 0.25 and 0.5 as well; see Fig. 4 (all methods give the same results). The results highlight the significant influence of frequency on the system response, which is to be expected (based on the 1D shear layer). For $\eta = 0.25$, the resonance spacing increases to 4, whereas for $\eta = 1.0$, it reduces to 1. In general, the spacing is approximately equal to $1/\eta$, which is to be expected based on the resonance condition (i.e., $\cos(k_S L) = 0$).

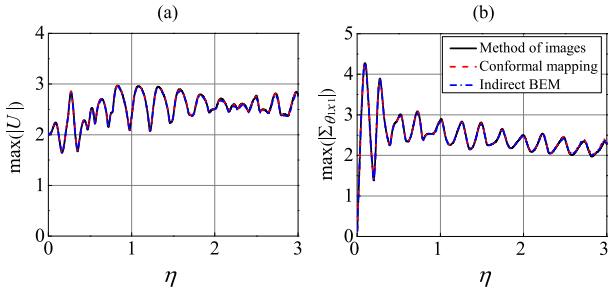

Fig. 2. Evaluation of the methods for the dimensionless frequency η: (a) anti-plane displacement at the ground surface U at $z = 0$, and (b) shear stress $\Sigma_{\theta_1 x_1}$ at $r_1 = R$.

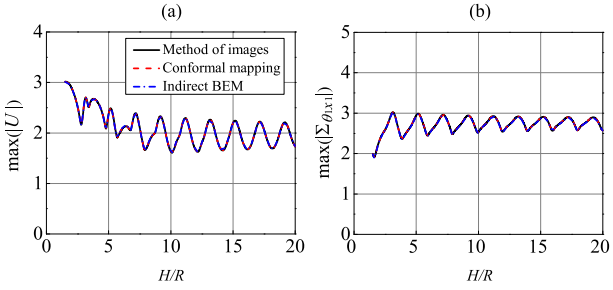

Fig. 3. Evaluation of the methods for the depth ratio H/R: (a) anti-plane displacement at the ground surface U at $z = 0$, and (b) shear stress $\Sigma_{\theta_1 x_1}$ at $r_1 = R$.

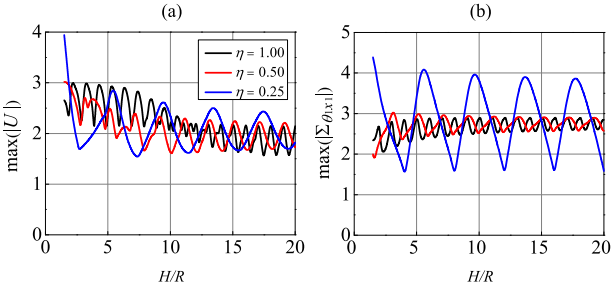

Fig. 4. Evaluation of the methods for the depth ratio H/R and for different frequencies: (a) anti-plane displacement at the ground surface U at $z = 0$, and (b) shear stress $\Sigma_{\theta_1 x_1}$ at $r_1 = R$.

5. Conclusions

The response of a cavity embedded in an elastic half-space subject to a harmonic SH wave has been examined in this study. To verify the accuracy of the method of conformal mapping and the indirect BEM, we compared those with the method of images (benchmark).

In a comprehensive evaluation, it was observed that both the method of conformal mapping and the indirect BEM perform accurately across the entire ranges of the dimensionless frequency and the embedded depth of the cavity. Therefore, we have successfully verified the accuracy of the method of conformal mapping and the indirect BEM. This is different from the 3D case [2], where converged results could not be obtained at high frequencies for the method of conformal mapping. The findings suggest that representing the waves scattered from the free surface by cylindrical waves (originating from an image

source of a priori unknown intensity) in the method of conformal mapping [2] is the cause of the inaccuracies at high frequency in the 3D problem. The cylindrical waves are probably not able to fully capture all wave conversions taking place at the free surface.

The evaluation revealed substantial influence of the dimensionless frequency and the embedded depth of the cavity on the responses at both the ground surface and the cavity surface. The system's response curves display nearly equally spaced resonances, which is in line with the resonances observed for the well-known one-dimensional shear layer subject to bedrock motion [8]. The system's response curves for the three-dimensional case [2] do not display such equally spaced resonances.

CRediT authorship contribution statement

Mingjuan Zhao: Writing – review & editing, Validation, Software, Methodology, Formal analysis. **João Manuel de Oliveira Barbosa:** Software, Methodology. **Andrei V. Metrikine:** Supervision, Methodology, Conceptualization. **Karel N. van Dalen:** Writing – review & editing, Supervision, Methodology, Conceptualization.

Declaration of competing interest

The authors declare that they have no known competing financial interests or personal relationships that could have appeared to influence the work reported in this paper.

Acknowledgements

We are grateful to the China Scholarship Council (CSC) (No. 201306110029) for the financial support of this work.

Data availability

Data will be made available on request.

References

[1] Stamos AA, Beskos DE. Dynamic analysis of large 3-D underground structures by the BEM. Earthq Eng Struct Dyn 1995;24(6):917–34.
[2] Zhao M, de Oliveira Barbosa JM, Metrikine AV, van Dalen KN. Semi-analytical solution for the 3D response of a tunnel embedded in an elastic half-space subject to seismic waves. Soil Dyn Earthq Eng 2023;174:108171.
[3] Achenbach JD. Wave propagation in elastic solids. Nord Holland Elsevier; 1973.
[4] Aki K, Richards PG. Quantitative seismology. University Science Books; 2002.
[5] Zhao M, de Oliveira Barbosa JM, Yuan J, Metrikine AV, van Dalen KN. Instability of vibrations of an oscillator moving at high speed through a tunnel embedded in soft soil. J Sound Vib 2021;494:115776.
[6] Liu Q, Zhao M, Wang L. Scattering of plane P, SV or Rayleigh waves by a shallow lined tunnel in an elastic half space. Soil Dyn Earthq Eng 2013;49:52–63.
[7] Luco JE, de Barros FCP. Dynamic displacements and stresses in the vicinity of a cylindrical cavity embedded in a half-space. Earthq Eng Struct Dyn 1994;23(3):321–40.
[8] Kramer SL. Geotechnical earthquake engineering. Pearson Education India; 1996.